Dielectric and electrothermal measurements on $(Cd_{0.83}Pb_{0.17})_2Nb_2O_7$ at liquid-nitrogen temperatures

W. N. Lawless and C. F. Clark
CeramPhysics, Inc., Westerville, Ohio 43081
(Received 12 January 1987)

The solid solution $(Cd_{0.83}Pb_{0.17})_2Nb_2O_7$ has a ferroelectric transition at 71 K. Dielectric, specific heat, and electrocaloric measurements are reported in the paraelectric phase of this material on multilayer ceramic capacitors which support electric field strengths up to 200 kV/cm. The experimental data are explained by a Ginzburg-Landau-Devonshire formalism with a single order parameter, indicating pure soft-mode behavior. A second-order phase transition is indicated, and the entropy of the transition is 0.58 cal $mol^{-1} K^{-1}$ estimated from the excess specific heat. Using the Curie constant determined from the dielectric data, an unusually large spontaneous polarization is found from the transition entropy, $P_s \sim 50\ \mu C/cm^2$.

INTRODUCTION

Ferroelectricity was discovered in pyrochlore $Cd_2Nb_2O_7$ over 30 years ago,[1] but the nature of ferroelectricity in this material still remains controversial. Early dielectric measurements on single crystals established the Curie point at 185 K and a second dielectric anomaly at 85 K, suggesting a second phase transition.[2] More recent studies suggest a *succession* of phase transitions, first to a ferroelastic phase, then to a ferroelectric phase, followed by a transition to an incommensurate phase below 80 K;[3] transitions between ferroelectric phases have also been reported.[4]

In contrast to the well-known perovskite structure (e.g., $BaTiO_3$), the pyrochlore structure (space group $Fd3m$) contains eight molecules per unit cell, and in the BO_6 oxygen octahedra the O-*B*-O chains follow zigzag lines along the ⟨110⟩ direction. The BO_6 octahedra are corner sharing, and the framework has the structure $(B_2O_6)_\infty$. Thus, it is not too surprising that the large number of degrees of freedom in the pyrochlore structure could lead to complex phase transitions in $Cd_2Nb_2O_7$.

The dominant transition (or concentration of transitions) in $Cd_2Nb_2O_7$ at 185–210 K can be suppressed to very low temperatures by solid solutions of Pb on the *A* site or Ta on the *B* site.[5] This has led to recent investigations of *quantum ferroelectricity* in the pyrochlore $(Cd,Pb)_2(Nb,Ta)_2O_7$ system.[6] Here it was found that quantum suppression of a phase transition is complete at 20 at.% Pb + 70 at.% Ta, and a temperature-independent dielectric constant is obtained below 15 K. However, in contrast to perovskite $KTaO_3$ and $SrTiO_3$, the dielectric data for this system do not follow the predictions of renormalization group theory.

These quantum-suppression effects in the pyrochlore $(Cd,Pb)_2(Nb,Ta)_2O_7$ system led to the development of a practical, *pressure-sensor* capacitor for cryogenic applications below 15 K—the capacitance is independent of temperature and magnetic field, and the reciprocal capacitance varies linearly with pressure.[7] Tape-cast, multilayer ceramic capacitors were developed for this sensor program, and this technology was used to fabricate the multilayer capacitor samples for the studies here.

It was observed in the $(Cd,Pb)_2(Nb,Ta)_2O_7$ ceramic system with transition temperatures below ~100 K that no *extraneous* transitions are present, and the dielectric constant is frequency-independent in the paraelectric phase, indicating pure soft-mode behavior.[8] Therefore, the complex phase transitions in $Cd_2Nb_2O_7$ near 200 K are apparently missing in the solid solutions with suppressed transition temperatures. The purpose of this paper is to report dielectric, specific heat, and electrocaloric measurements on one of these simple solid solutions to explore the expected soft-mode behavior and the nature of this transition. Specifically, the $(Cd_{0.83}Pb_{0.17})_2Nb_2O_7$ system with $T_c = 71$ K was chosen for study because of the convenience of using liquid nitrogen (77.4-K boiling point). Dense, tape-cast, multilayer capacitors were measured because of the large electric field strengths possible with these structures compared to either ceramic or single-crystal samples.

Electrocaloric measurements are a sensitive test of pure soft-mode behavior in the paraelectric state because the Ginzburg-Landau-Devonshire formalism with a single order parameter is used to analyze both dielectric and electrocaloric data provided the specific heat is known. Similar measurements on $KTaO_3$ and $SrTiO_3$ at helium temperatures have been published elsewhere.[9]

EXPERIMENTAL METHODS AND RESULTS

Reagent-grade powders of CdO, PbO, and Nb_2O_5 were mixed and calcined, and these powders were ground and recalcined to insure complete reaction. Final powders were ground to 1-μm particle size, and a tape was prepared using an appropriate organic binder. An electroding paste (40 wt.% Pt, 20 wt.% Pd, 40 wt.% Au) was silk-screened between tape sections, and the tape stack was sintered at 1230 °C for $\frac{1}{2}$ h following binder burnout. The techniques here were developed earlier,[7] as mentioned above. The resulting multilayer capacitors were $1 \times 1 \times 0.2$ cm^3 and contained 46 ceramic layers with

 ©1987 The American Physical Society

electrodes and the layer thickness was 0.0045 cm. In addition, a ceramic sample was fabricated without internal electrodes for accurate dielectric measurements (at zero electric field). This sample had nichrome-gold electrodes evaporated on the major faces. For all samples studied here, the densities were about 95% of the theoretical density.

Dielectric measurements

All capacitance measurements were made with a General Radio 1620-A transformer ratio-arm bridge with associated oscillator and detector. Since the multilayer capacitors had capacitance values ~ 4.3 μF at 77 K, a General Radio 1615-P1 range extender capacitor was employed. For electric-field measurements a Keithley Model 247 high-voltage power supply was used, and a special bridge-protection system[10] was built for extending the bridge measurements above 500 V.

Three terminal measurements with coaxial cables were made, and two types of measurements were conducted: (1) $\epsilon(E)$ measurements on multilayer capacitors immersed in liquid nitrogen; and (2) $\epsilon_0(T)$ measurements on the ceramic sample without internal electrodes. The latter measurements were made in a double-can cryostat outfitted with a temperature-controlled inner can.

Dielectric data at zero field, $\epsilon_0(T)$, measured on the ceramic sample from 65 to 105 K are shown in Fig. 1. A large maximum in ϵ_0 (6620) occurs at 71 K, and there is no dielectric evidence for additional transitions in this temperature range. Measurements of the frequency dependence of ϵ_0 at 77 K (not shown) revealed negligible changes in ϵ_0 in the range 50 Hz to 100 kHz.

At temperatures above 85 K in Fig. 1, the data follow a Curie-Weiss law, $\epsilon_0 = c/(T - T_0)$, with $c \simeq 2.5 \times 10^5$ and $T_0 \simeq 43$ K.

The electric field dependence of the dielectric constant ϵ_E is shown in Fig. 2, measured at 77 K on two multilayer-capacitor samples up to 200 kV/cm. Data were measured on both increasing and decreasing E. There is excellent agreement between the two data sets, and there is no evidence of hysteretic behavior in these dielectric data (nor in the electrocaloric data, see below).

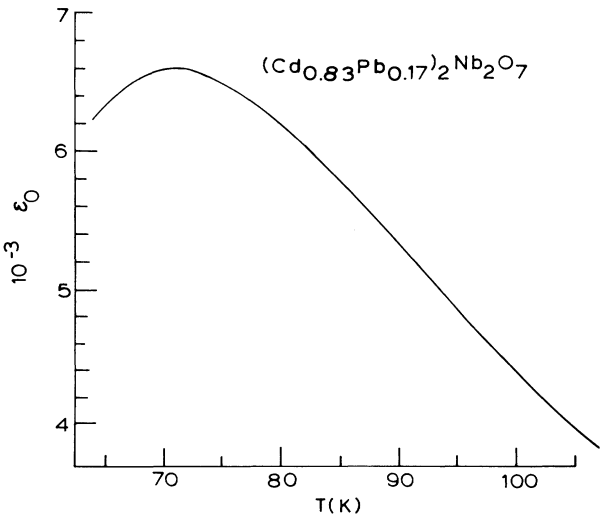

FIG. 1. Zero-field dielectric constant data measured on the ceramic sample without internal electrodes.

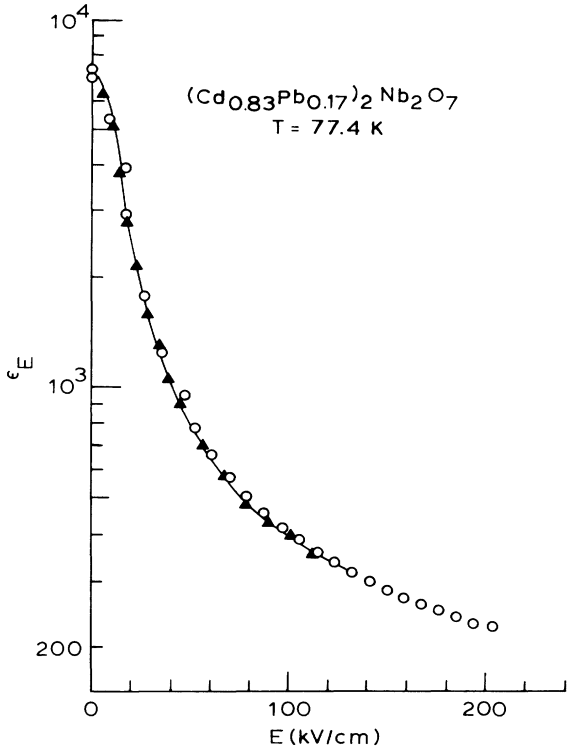

FIG. 2. Electric field dependence of the dielectric constant measured on two multilayer capacitor samples immersed in liquid nitrogen. The curve shown is the fit up to 120 kV/cm discussed in the text.

Specific-heat and electrocaloric measurements

For these electrothermal measurements the multilayer-capacitor samples were mounted as shown in Fig. 3. The sample (A) is attached to a temperature-controlled reservoir (B) by a long-time-constant thermal link (D) indium-soldered to a copper mounting pin (C), and the sample is in a very high vacuum. This arrangement not only ensures nearly adiabatic conditions during field pulsing but also minimizes the addenda corrections that enter both the specific heat and electrocaloric measurements (see below). The sample is outfitted with a carbon-chip thermometer ~ 10 mg (E), a Manganin heater (F), and a high-voltage lead (G). The reservoir (B) is at ground potential, and all connections to the internal Pt-Pd-Au electrodes were made with fired silver paste. To ensure that all electrodes were contacted, the capacitance of the sample in the Fig. 3 arrangement was always measured after cooldown in the calorimeter.

The reservoir post (B) in Fig. 3 is mounted in a double-can adiabatic calorimeter described elsewhere.[11] The adiabatic shield was lined with aluminized Mylar to eliminate radiation effects, and the bottom of the outer

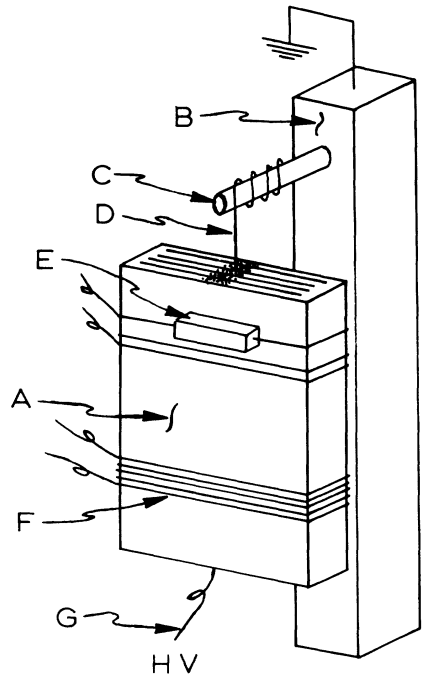

FIG. 3. Experimental arrangement for measuring electrothermal data on a multilayer capacitor (*A*) outfitted with a thermometer (*E*) and heater (*F*) and suspended on a long-time-constant thermal link (*D*) from a pin (*C*) mounted in a temperature-controlled reservoir (*B*). The reservoir is at ground potential, and the lower end of the sample has a high-voltage lead (*G*).

can contained zeolites to achieve a hard vacuum. The carbon-chip thermometer, *E* in Fig. 3, was calibrated *in situ* against a calibrated Pt thermometer mounted in the reservoir. All thermometer voltages and exciting currents were measured using Keithley Model 181 nanovoltmeters.

Two types of specific-heat (*C*) measurements were made. First, the zero-field specific heat C_0 was measured by the dynamic pulse method.[11] Next, for the field-dependent specific heat C_E, a "drift" method was used, as follows: The sample heater is used to heat the sample to an elevated temperature (e.g., 100 K), and after deactivating the heater the sample temperature decays back to the reservoir temperature. Measurement of the decay rate dT/dt is then a measurement of C_E. The C_0 data from the pulse method are needed to calibrate the thermal link, and the details of this drift method have been described previously.[12] In the drift measurements here, the experimental quantities were measured on the nanovoltmeters interfaced with a Digital Equipment Corp. DEC 350 computer through IEEE interfaces, and the computer was programmed to read the voltmeters every 10 s.

The electrocaloric measurements consisted of measuring the sample temperature as the field was cycled $0 \rightarrow E \rightarrow 0$, and this was accomplished by monitoring the changes in the thermometer voltage on a strip chart recorder. A Keithley Model 247 high-voltage power supply was used, and a voltage switching circuit was built which allowed the rapid charging and discharging of the capacitor (i.e., limited only by the *R-C* time constant of the capacitor circuit). That is, rapid charging and discharging are important to maintain nearly adiabatic conditions, but the discharge through the power supply had a long time constant. Also, use of this switching circuit permitted a preset voltage level to be applied to the sample.

The addenda corrections enter both the specific-heat and electrocaloric measurements. The addenda are the thermometer, heater, varnish, etc. fixtured on the sample as shown in Fig. 3 (determined by cumulative weighings), and the total heat capacity $\mathcal{C}$ is given by

$$\mathcal{C} = mC + \mathcal{C}_a \ , \tag{1}$$

where m and C are the mass and specific heat of the sample, respectively, and $\mathcal{C}_a$ is the heat capacity of the addenda. This latter heat capacity was determined using literature tables[13] for the specific heats of the addenda.

A subtlety is involved in reducing the *E*-field-dependent specific heat C_E. Namely, a substantial portion ($\sim 40\%$) of the ceramic material in the multilayer capacitor is *not* exposed to the electric field, and this inactive ceramic material enters Eq. (1) as an addenda contribution. The ceramic involved is easily determined from the geometry of the capacitor, and the measured zero-field specific heat is used to make this correction.

In an electrocaloric event, the actual temperature change of the active ceramic, ΔT_{act}, is related to the measured change, ΔT_{meas}, by[14]

$$\Delta T_{\text{act}} = \Delta T_{\text{meas}}(1 + \mathcal{C}_a / mC_E) \ . \tag{2}$$

Here also the inactive ceramic material enters into the addenda term in Eq. (2).

As a final consideration, an electrocaloric ΔT in general has two components—a reversible component, ΔT_r, and a hysteretic component, ΔT_h. These components are easily separable by assuming that ΔT_h does not depend on the sign of ΔE.[14] However, in all cases here the ΔT's were perfectly reversible on cycling $0 \rightarrow E \rightarrow 0$, indicating that the hysteretic components are negligible.

Zero-field specific-heat data measured by the pulse method are shown in Fig. 4. The addenda in these data according to Eq. (1) constituted 9–10 % of the total heat capacity. Two capacitors were measured, and the agreement between the two data sets in Fig. 4 is very good. An *excess* specific heat is apparent in the measured data. The C_0 data below 72 K and above 100 K approximately follow the Debye specific-heat function[15] with $\Theta_D = 442$ K, as indicated in Fig. 4. Using this as the background specific heat, the excess zero-field specific heat ΔC_0 can be determined, and these data are shown in the upper portion of Fig. 4. The ΔC_0 data display a maximum at 82 K, about 11 K higher than the temperature of the dielectric constant maximum (Fig. 1), but the position of this ΔC_0 maximum depends on the choice of the background specific heat.

The electric field dependence of the specific heat C_E was measured at several field levels up to 180 kV/cm by the drift method described above, and these data are shown in Fig. 5 plotted as C_E/C_0 versus E at four tem-

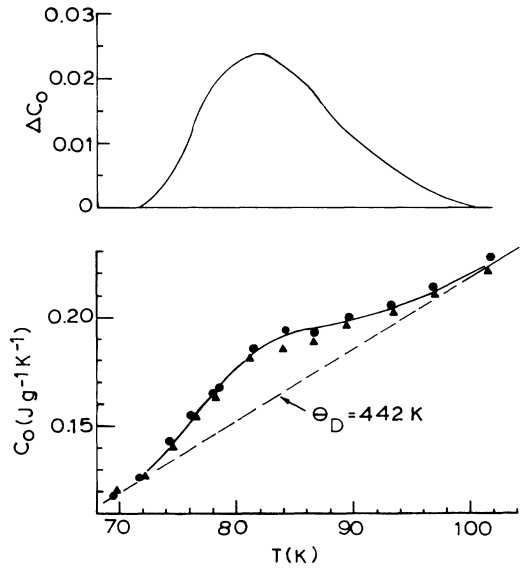

FIG. 4. Zero-field specific-heat measurements made on two capacitor samples. An excess specific heat appears above a background specific heat (effective $\Theta_D = 442$ K) and indicates a second-order transition. The upper plot shows the subtracted excess specific heat.

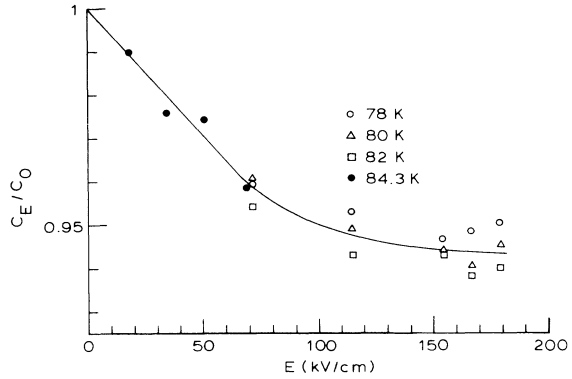

FIG. 5. Electric field dependence of the specific heat in the paraelectric phase measured on capacitors by a drift method. Plotting the data as C_E/C_0 apparently removes the temperature dependence, and up to 180 kV/cm, $C_E/C_0 \geq 94.5\%$.

peratures. Three capacitors were measured, and the agreement between the data sets is very good. It is also satisfying that the ratio C_E/C_0 approaches unity at $E \rightarrow 0$ since the corrections here include the inactive ceramic and are rather large ($\sim 50\%$).

A universal temperature behavior for C_E/C_0 in the temperature range 78–84 K is suggested by the data in Fig. 5, and this is the temperature range of the maximum in ΔC_0 in Fig. 4. The C_E/C_0 data decrease linearly with E up to ~ 100 kV/cm, above which C_E/C_0 is approximately constant at 94.5% (or drops more slowly with E—a semilog plot of the C_E/C_0 data strongly suggests the latter). At 82 K the excess specific heat at zero field ΔC_0 constitutes about 12% of the total specific heat C_0. One suspects that at sufficiently large fields this excess specific heat would be quenched.

It is significant that both ϵ_E in Fig. 2 and C_E/C_0 in Fig. 5 begin to show saturation effects at ~ 200 kV/cm.

These drift experiments serve another very useful purpose; namely, the detection of a *latent heat* associated with a first-order phase transition. Referring to Fig. 3, if a latent heat were released, this heat would be dissipated through the long-time-constant thermal link (D), and the sample temperature would stabilize until the heat was dissipated, causing $dT/dt = 0$. This phenomenon is unmistakable in a drift experiment, and no evidence of a latent heat was observed in these drift experiments (note that a drift at $E = 0$ was required to calibrate the thermal link).[12] Therefore, the evidence is consistent with a second-order phase transition in $(Cd_{0.83}Pb_{0.17})_2Nb_2O_7$.

In the electrocaloric experiments, polarization heating and depolarization cooling take place, and as mentioned above the ΔT's on heating and cooling were identical within the experimental uncertainty ($\sim \pm 10$ mK) in the paraelectric state. Depolarization-cooling effects are thermodynamically consistent with $d\epsilon_0/dT < 0$ (Fig. 1) and $C_E/C_0 < 1$ (Fig. 5).

The reduction of the electrocaloric data follows Eq. (2), and it is clear that the specific-heat data above are needed for these reductions. The C_E/C_0 data in Fig. 5 were assumed temperature independent in reducing the electrocaloric data, but this is not a large effect ($C_E/C_0 \geq 95\%$). Electrocaloric data measured on two capacitors at 77.7 and 94.3 K up to 130 kV/cm are shown in Fig. 6. The capacitors tended to fail dielectrically under rapid field switching, and the data in Fig. 6 represent the highest E fields achieved.

The ΔT_r values in Fig. 6 range up to ~ 1 K, and two regions are indicated: A low-field E^2 region, and a high-field E^{6+2n} region.

DATA ANALYSES

In this section we first consider a Ginzburg-Landau-Devonshire (GLD) analysis of the experimental data coupled with the TdS equation for dielectric materials. The motivation here is to see if a single-order-parameter analysis can explain the dielectric and thermal data, thereby indicating soft-mode behavior in this material. This type of analysis proved successful in explaining similar data measured on the soft-mode perovskites $KTaO_3$ and $SrTiO_3$ at liquid-helium temperatures.[14,16]

In the GLD formalism, the polarization P is the order parameter, and the free energy is expanded in powers of P,

$$A = A_0 + \tfrac{1}{2}\chi_0 P^2 + \tfrac{1}{4}\xi P^4 + \tfrac{1}{6}\zeta P^6 + \cdots , \tag{3}$$

where χ_0 is assumed to be the only temperature-dependent coefficient,[17] and the coefficients ξ and ζ are the appropriately averaged coefficients for a ceramic material. This expansion has the definitional properties that

$$E = \frac{\partial A}{\partial P}, \quad \chi_E = \frac{4\pi}{\epsilon_E} = \frac{\partial^2 A}{\partial P^2} . \tag{4}$$

Performing the second derivative in Eq. (4) and inverting the first derivative to obtain $P(E)$, we have[14]

$$\chi_E=\chi_0+(3\xi/\chi_0^2)E^2+(5\zeta/\chi_0^4-6\xi^2/\chi_0^5)E^4+\cdots , \quad (5)$$

which we shall use below to analyze the ϵ_E data in Fig. 2.

The TdS equation for dielectrics (i.e., paraelectrics which do not have a spontaneous polarization) is given by[18]

$$TdS=mC_E dT+vT\left[\frac{\partial P}{\partial T}\right]_E dE , \quad (6)$$

where m and v are the sample mass and volume, respectively. Under adiabatic conditions ($dS=0$) and assuming both that $\Delta T_r/T$ is relatively small (e.g., Fig. 6) and that C_E is weakly field dependent (e.g., Fig. 5), Eq. (6) becomes

$$\rho C_E\frac{\Delta T_r}{T}=-\int_0^E\frac{\partial P}{\partial T}dE . \quad (7)$$

Using the $P(E)$ inversion above, performing $\partial P/\partial T$ and integrating, Eq. (7) becomes[14]

$$\rho C_E\frac{\Delta T_r}{T}=aE^2+bE^4+cE^6+\cdots , \quad (8)$$

where

$$a=\dot{\chi}_0/2\chi_0^2 ,$$
$$b=-\xi\dot{\chi}_0/\chi_0^5 , \quad (9)$$
$$c=21\xi^2\dot{\chi}_0/6\dot{\chi}_0^8-\zeta\dot{\chi}_0/\chi_0^7 .$$

In arriving at Eqs. (8) and (9), ξ and ζ are assumed temperature independent and $\dot{\chi}_0=d\chi_0/dT=-(4\pi/\epsilon_0^2)(d\epsilon_0/dT)$.

Turning to the experimental data, we first fit the ϵ_E data in Fig. 2 to Eq. (5), rewritten as

$$4\pi/\epsilon_E=4\pi/\epsilon_0+\sum_1^4 E^{2n} , \quad (10)$$

and the fitting parameters for this fit are given in Table I where the E fields are in statvolt/cm and the b_n coefficients are in the cgs (esu) system (in all these data fittings, $E\leq 120$ kV/cm, the largest common field strength). This fit to the ϵ_E-E data is shown by the solid curve in Fig. 2, and it was found that the $n=4$ fit yielded an excellent fit to the data (i.e., the fit improved substantially from $n=3$).

Next, the ΔT_r data in Fig. 6 are fitted to Eq. (8) rewritten as (see below for the order of this fit),

$$\Delta T_r=\sum_1^5 a_{n-1}E^{2n} , \quad (11)$$

and these a_n coefficients are given in Table II, also in the cgs (esu) system. These fits are shown by the solid curves in Fig. 6, and here the fifth-order fit of Eq. (11) gave an excellent fit to the data (compared to the fourth-order fit). The procedure now is to correlate the respective coefficients in Eqs. (10) and (11). First, however, we address the consistency of the fourth- and fifth-order expansions used in these equations, since the coefficients in Tables I and II depend on the order of the fits. These two fits are commensurate for the following reason: The susceptibility χ involves the second derivative, Eq. (4), whereas the polarization P involves the first derivative, and ΔT_r involves an integration over E, Eq. (7). Thus, an E^m expansion for ΔT_r is equivalent to an E^{m-2} expansion for χ.

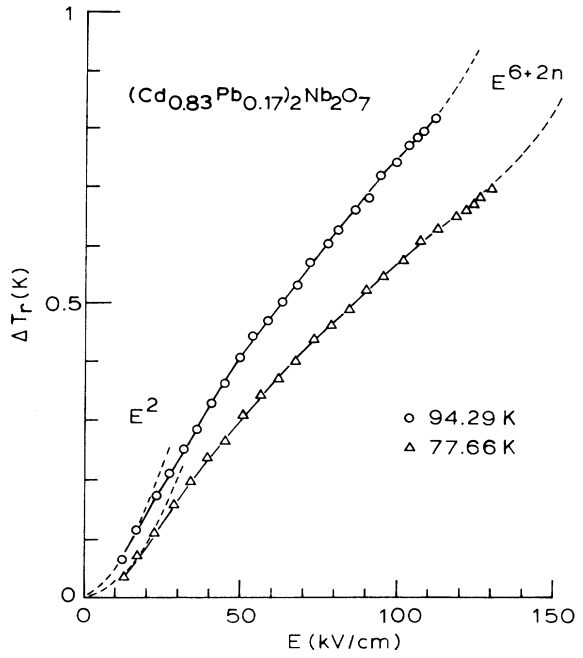

FIG. 6. Electrocaloric data (polarization heating, depolarization cooling) measured on ceramic capacitors in the paraelectric phase. The electrocaloric effects are perfectly reversible on field cycling. The curves shown result from the fits discussed in the text. At low fields, the E^2 dependence is indicated, and at large fields the E^{6+2n} terms become important.

Since the specific heat is weakly field dependent, Fig. 5, we will approximate $C_E\simeq C_0$ in Eq. (8), and comparing Eqs. (8), (9), and (11) we find

$$\dot{\chi}_0/2\chi_0^2=(\rho C_0/T)a_0 . \quad (12)$$

At 77.7 and 94.3 K, the a_0 parameters are given in Table II, χ_0 data are given in Fig. 1, C_0 data are given in Fig. 4, and the measured density is $\rho=6.28$ g cm^{-3}. Substituting in Eq. (12) we find that $d\epsilon_0/dT=-82$ and -150 K^{-1} at 77.7 and 94.3 K, respectively. For comparison, from Fig.

TABLE I. $\epsilon(E)$ fitting parameters at 77 K, according to Eq. (10); data from Fig. 2 fitted.

Parameter	Value
b_1	4.302×10^{-7}
b_2	-2.097×10^{-12}
b_3	5.253×10^{-18}
b_4	-4.767×10^{-24}

TABLE II. $\Delta T_r(E)$ fitting parameters in cgs(esu) units, according to Eq. (11); data from Fig. 6 fitted.

Parameter	77.66 K	94.29 K
a_0	2.513×10^{-5}	4.315×10^{-5}
a_1	-7.643×10^{-10}	-1.997×10^{-9}
a_2	1.133×10^{-14}	4.297×10^{-14}
a_3	-7.204×10^{-20}	-3.887×10^{-19}
a_4	1.614×10^{-25}	1.226×10^{-24}

$1\ d\epsilon_0/dT=-73$ and $-110\ \mathrm{K}^{-1}$, respectively, in reasonably good agreement considering the assumptions and approximations employed.

Again comparing Eqs. (8), (9), and (11) for the next-higher-order coefficients, we have for the electrothermal case,

$$-\xi\dot{\chi}_0/\chi_0^5=(\rho C_0/T)a_2\ , \tag{13}$$

and proceeding as above using $d\epsilon_0/dT$ data from Fig. 1, we have (cgs)

$$\begin{aligned}\xi(77.7\ \mathrm{K})&=2.69\times10^{-13}\ ,\\ \xi(94.3\ \mathrm{K})&=3.63\times10^{-13}\ .\end{aligned} \tag{14}$$

Next, from the ϵ_E expansion, Eq. (10),

$$3\xi/\chi_0^2=b_1 \tag{15}$$

on comparing with Eq. (5), and from Table I and Fig. 1 we find (cgs)

$$\xi(77.4)=4.31\times10^{-13}\ . \tag{16}$$

The agreement here between the ξ values from the electrocaloric and specific-heat data, Eq. (14), and the dielectric data, Eq. (16), is very good considering the large amount of experimental data employed [note that Eq. (14) suggests a positive temperature dependence for ξ that has been ignored in arriving at Eqs. (8) and (9)]. Adopting the average value for ξ (cgs) from Eqs. (14) and (16),

$$\xi=(3.54\pm0.81)\times10^{-13}\ , \tag{17}$$

and the sign of ξ indicates a second-order transition for the ceramic.

Turning next to the ζ coefficient, for the electrothermal case

$$21\xi^2\dot{\chi}_0/6\chi_0^8-\zeta\dot{\chi}_0/\chi_0^7=(\rho C_0/T)a_2\ , \tag{18}$$

which yields (cgs)

$$\begin{aligned}\zeta(77.7\ \mathrm{K})&=2.48\times10^{-22}\ ,\\ \zeta(94.3\ \mathrm{K})&=1.64\times10^{-22}\ .\end{aligned} \tag{19}$$

For the dielectric case,

$$5\zeta/\chi_0^4-6\xi^2/\chi_0^5=b_2\ , \tag{20}$$

which yields (cgs)

$$\zeta(77.4\ \mathrm{K})=0.86\times10^{-22}\ . \tag{21}$$

Once again, there is satisfactory agreement between the electrocaloric, specific heat, and dielectric data [note in particular the high powers of χ_0 entering Eqs. (18) and (20)], and the average value of ζ is

$$\zeta=(1.66\pm0.18)\times10^{-22}\ . \tag{22}$$

This procedure can be continued by taking higher-order terms in Eq. (3), following through the derivations, and combining with the a_3, b_3, etc., coefficients in Tables I and II, but this will not be pursued here.

Turning next to the excess-specific-heat data, ΔC_0 in Fig. 4, this is indicative of a second-order phase transition, and the entropy of the transition is easily found by integrating the ΔC_0 data,

$$\Delta S\simeq0.58\ \mathrm{cal\ mol^{-1}\,K^{-1}}\ . \tag{23}$$

Applying the well-known relation $\Delta S=2\pi P^2/c$, where P is the spontaneous polarization near the transition and c is the Curie constant (2.5×10^5, see above), we find

$$P\simeq50\ \mu\mathrm{C/cm^2}\ . \tag{24}$$

which is a very large value (see below). We point out that this result strongly depends on the assignment of the *background* specific heat in Fig. 4, but a very large spontaneous polarization is clearly indicated.

CONCLUSIONS AND DISCUSSION

A substantial amount of dielectric, specific heat, and electrocaloric data are reported for $(Cd_{0.83}Pb_{0.17})_2Nb_2O_7$ in the temperature range 70–120 K and at electric field strengths up to 200 kV/cm. Multilayer ceramic capacitors were measured which allowed such large field strengths. The experimental data up to 120 kV/cm can be explained and correlated very well by the GLD formalism with a single order parameter, Eq. (3), in combination with the TdS equation for paraelectrics, Eq. (6). Presumably the uncertainties in ξ and ζ, Eqs. (17) and (22), could be reduced by including a T dependence of ξ, but this was not pursued.

What is clear is that the success of the simple GLD formalism in correlating this large amount of data at large field strengths demonstrates that $(Cd_{0.83}Pb_{0.17})_2Nb_2O_7$ with $T_c=71$ K exhibits pure soft-mode behavior in the paraelectric state, as first suggested by the frequency-independence of ϵ.[8] Additionally, the constellation of phase transitions seen in pure $Cd_2Nb_2O_7$ at 185–210 K is missing in this case.

The ξ and ζ coefficients above agree in magnitude with those determined for $BaTiO_3$ (-1.0×10^{-13} and 5.4×10^{-22}, respectively),[19] but are considerably smaller than those for $KTaO_3$ ($\sim10^{-11}$ and $\sim10^{-19}$) and $SrTiO_3$ ($\sim10^{-11}$ and $\sim10^{-21}$).[14,16]

A second-order transition in the ceramic is indicated by the sign of ξ, Eq. (17), in agreement with the absence of a latent heat observed in the specific-heat drift measurements. In addition, the excess specific heat in Fig. 4 is consistent with a second-order transition. However, the order of the transition in a *single crystal* may be different than in the ceramic due to the elastic boundary conditions in the latter case.

The behavior of $(Cd_{0.83}Pb_{0.17})_2Nb_2O_7$ is markedly different from $Cd_2Nb_2O_7$, although there is no doubt that both materials have the $Fd3m$ pyrochlore structure: A very large Curie constant is found from the Fig. 1 data, $c \simeq 2.5 \times 10^5$, compared to $c \simeq 7 \times 10^4$ for $Cd_2Nb_2O_7$.[2] The transition entropy calculated from Fig. 4, $\Delta S \simeq 0.58$ cal mol^{-1} K^{-1}, is huge compared to that for $Cd_2Nb_2O_7$, $\Delta S \simeq 0.01$ cal mol^{-1} K^{-1}.[20] And from this entropy a spontaneous polarization $P \sim 50$ μC/cm^2 is estimated which is about an order of magnitude larger than that for $Cd_2Nb_2O_7$, ~ 6 μC/cm^2.[5] We remark that in fact *all* these quantities (c, ΔS, P) are *larger* than those found in displacive ferroelectrics in general such as $BaTiO_3$, $LiNbO_3$, etc. (e.g., $c \lesssim 2 \times 10^5$, $\Delta S \lesssim 0.3$ cal mol^{-1} K^{-1}, $P \lesssim 30$ μC/cm^2).

There is some additional evidence that the dielectric properties of $Cd_2Nb_2O_7$ are enhanced by solid solutions on the A or B sites. Pyroelectric measurements[21] yielded a spontaneous polarization ~ 15 μC/cm^2 for a $(Cd,Pb)_2(Nb,Ta)_2O_7$ ceramic sample at cryogenic temperatures, compared to 4–6 μC/cm^2 measured on a similarly prepared $Cd_2Nb_2O_7$ sample in the same temperature range. One can speculate that the removal of extraneous transitions and the occurrence of pure soft-mode behavior induced by these solid solutions in $Cd_2Nb_2O_7$ causes the enhanced dielectric properties, and single-crystal studies here may be particularly illuminating.

ACKNOWLEDGMENTS

The authors are indebted to J. V. Biggers and G. O. Dayton for preparation of the ceramic samples and to R. W. Arenz for technical assistance.

[1]W. R. Cook, Jr. and H. Jaffe, Phys. Rev. **88**, 1426 (1952); **89**, 1297 (1953).
[2]G. Shirane and R. Pepinsky, Phys. Rev. **92**, 504 (1953); J. K. Hulm, *ibid.* **92**, 504 (1953).
[3]See N. N. Kolpakova, B. Brezina, and E. S. Sher, Jpn. J. Appl. Phys. **24**, 823 (1985) and references therein.
[4]See G. A. Smolensky, N. N. Krainik, L. S. Kamzina, F. M. Salaev, E. A. Tarakanov, and E. S. Sher, Jpn. J. Appl. Phys. **24**, 820 (1985), and references therein.
[5]F. Jona, G. Shirane, and R. Pepinsky, Phys. Rev. **98**, 903 (1955).
[6]C. F. Clark, W. N. Lawless, and A. S. Bhalla, Jpn. J. Appl. Phys. **24**, 266 (1985).
[7]W. N. Lawless, C. F. Clark, and G. A. Samara, Rev. Sci. Instrum. **56**, 1913 (1985).
[8]C. F. Clark and W. N. Lawless (unpublished).
[9]W. N. Lawless, Phys. Rev. B **16**, 433 (1977); Ferroelectrics **15**, 159 (1977).
[10]W. Schulze, Ph.D. thesis, Pennsylvania State University, State College, Pennsylvania, 1974.
[11]W. N. Lawless, Phys. Rev. B **14**, 134 (1976).
[12]W. N. Lawless, C. F. Clark, and R. W. Arenz, Rev. Sci. Instrum. **53**, 1647 (1982).
[13]R. J. Corruccini and J. J. Gniewek, Natl. Bur. Stand. (U.S.) Monogr. **21**; J. T. Heessels, Cryogenics **11**, 483 (1971).
[14]W. N. Lawless, Phys. Rev. B **16**, 433 (1977).
[15]E. S. R. Gopal, *Specific Heats at Low Temperatures* (Plenum, New York, 1966).
[16]W. N. Lawless, Ferroelectrics **15**, 159 (1977); Phys. Rev. B **18**, 2394 (1978).
[17]See A. F. Devonshire, Adv. Phys. **3**, 85 (1954); W. R. Buessem, L. E. Cross, and A. K. Goswami, J. Am. Ceram. Soc. **49**, 33 (1966).
[18]W. N. Lawless, J. Phys. Chem. Solids **30**, 1161 (1969).
[19]F. Jona and G. Shirane, *Ferroelectric Crystals* (Pergamon, New York, 1962).
[20]H. Danner and R. Pepinsky, Phys. Rev. **99**, 1215 (1955).
[21]C. F. Clark, W. N. Lawless, and A. S. Bhalla, Jpn. J. Appl. Phys. **24**, 266 (1985).